

# Generic Mechanism of Optimal Energy Transfer Efficiency: A Scaling Theory of the Mean First Passage Time in Exciton Systems

Jianlan Wu,<sup>1,2</sup> Robert J. Silbey\*,<sup>1</sup> and Jianshu Cao<sup>†1</sup>

<sup>1</sup>*Department of Chemistry, MIT, 77 Massachusetts Ave, Cambridge, MA, 02139, USA*

<sup>2</sup>*Physics Department, Zhejiang University,  
38 ZheDa Road, Hangzhou, Zhejiang, 310027, China*

(Dated: July 26, 2021)

## Abstract

An asymptotic scaling theory is presented using the conceptual basis of trapping-free subspace (i.e., orthogonal subspace) to establish the generic mechanism of optimal efficiency of excitation energy transfer (EET) in light-harvesting systems. Analogous to Kramers' turnover in classical rate theory, the enhanced efficiency in the weak damping limit and the suppressed efficiency in the strong damping limit define two asymptotic scaling regimes, which are interpolated to predict the functional form of optimal efficiency of the trapping-free subspace. In the presence of static disorder, the scaling law of transfer time with respect to dephasing rate changes from linear to square root, suggesting a weaker dependence on the environment. Though formulated in the context of EET, the analysis and conclusions apply in general to open quantum processes, including electron transfer, fluorescence emission, and heat conduction.

---

\* Dedicated to the memory of Prof. Robert J. Silbey

† Electronic address: jianshu@mit.edu

The optimization of the excitation energy transfer (EET) process presents a challenge for understanding photosynthetic systems as well as for designing efficient solar energy devices. Multi-dimensional spectra have allowed detailed probes of EET dynamics, revealing signatures of quantum coherence [1–4]. In contrast to the common belief that noise retards motion and coherence enhances mobility, the EET efficiency can be optimized at an intermediate level of noise, leading to the notion of noise-enhanced energy transfer [5–10]. Fermi’s golden rule rate provides a simple interpretation and suggests that stochastic resonance between the donor and acceptor enhances EET efficiency [8–10]. Another possible mechanism is that noise suppresses destructive interference between pathways [8, 9]. The situation is further complicated by the findings that initial preparation, coherence of incident photons, site energy, spatial correlation, static disorder, and various approximations invoked in quantum master equations can all play a role in establishing optimal efficiency [10–15]. Therefore, a general mechanism for optimization in an arbitrary EET system accompanying all these effects is clearly needed but has not yet been formulated.

In this Letter, we utilize the concept of trapping-free subspace (i.e., orthogonal subspace) to bring together all of the above considerations into a unified framework, that allows us to establish asymptotic scaling relations under both dynamic and static disorder and identify the generic behavior of optimal EET efficiency. The definition of a trapping-free subspace is a generalization of the invariant subspace [8] and is closely related to the concept of decoherence-free subspace in quantum information [16].

*Model.* — We consider a light-harvesting EET system (see examples in Fig. 1) described by the quantum master equation for the reduced density matrix of the single excitation manifold [9],

$$\dot{\rho}(t) = -\mathcal{L}\rho(t). \quad (1)$$

Here, the Liouville superoperator  $\mathcal{L} = \mathcal{L}_{\text{sys}} + \mathcal{L}_{\text{dissip}} + \mathcal{L}_{\text{trap}} + \mathcal{L}_{\text{decay}}$  comprises four terms, each describing a distinct dynamic process: (i)  $\mathcal{L}_{\text{sys}}\rho(t) = (i/\hbar)[H_S, \rho(t)]$ , the dynamics of the isolated system, where  $H_S$  is the system Hamiltonian; (ii)  $\mathcal{L}_{\text{dissip}}$ , the exciton redistribution and dephasing within the single-excitation manifold due to the interaction with the surrounding environment; (iii)  $\mathcal{L}_{\text{trap}}$ , the trapping of excitation energy at the reaction center for the production of chemical energy; (iv)  $\mathcal{L}_{\text{decay}}$ , the decay of the excitation energy to ground state in the form of heat or a photon. The Liouville superoperator  $\mathcal{L}$  becomes

invertible because of the two irreversible energy depletion terms,  $\mathcal{L}_{\text{trap}}$  and  $\mathcal{L}_{\text{dissp}}$ . A basic property of an EET system is its energy transfer efficiency,

$$q = \text{Tr} \int_0^\infty \mathcal{L}_{\text{trap}} \rho(t) dt, \quad (2)$$

where  $\text{Tr}$  denotes the trace over states. For an efficient EET system such as a light-harvesting protein complex, its nearly unit energy transfer efficiency,  $q \sim 1$ , implies a clear time-scale separation between the decay process and the trapping process. Under this condition and with a homogeneous decay rate  $k_d$ , the transfer efficiency is given, to a good approximation [9], by

$$q \approx \frac{1}{1 + k_d \langle t \rangle}, \quad (3)$$

where  $\langle t \rangle = \text{Tr} [\mathcal{L}_0^{-1} \rho(0)]$  is the the average trapping time for the initial density matrix  $\rho(0)$ , and  $\mathcal{L}_0 = \mathcal{L}_{\text{sys}} + \mathcal{L}_{\text{trap}} + \mathcal{L}_{\text{dissip}}$  is the new Liouville superoperator in the absence of decay.

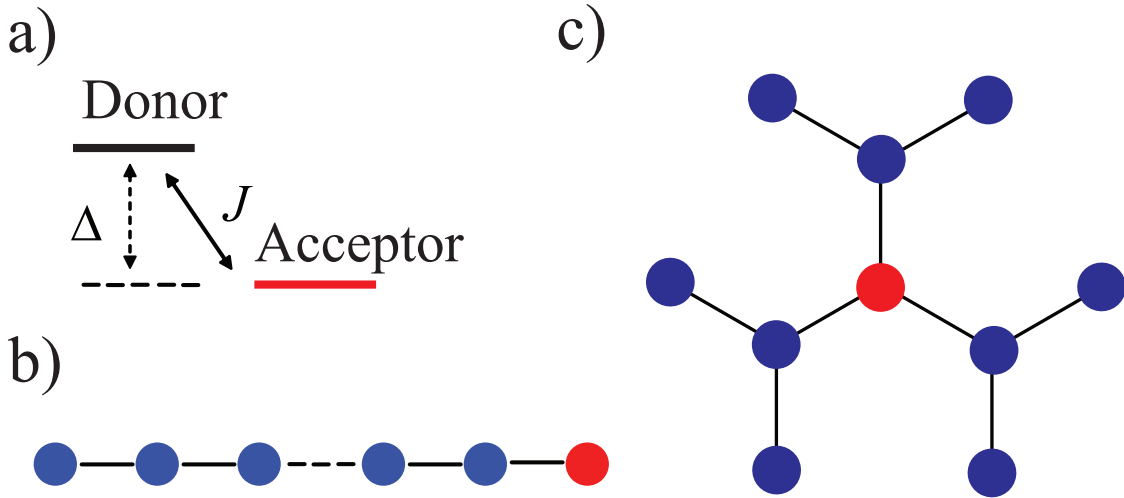


FIG. 1: (color online) Various EET systems with the trapping free subspace: a) A donor-acceptor system with an energy mismatch  $\Delta$  larger than the site-site coupling  $J$  ( $\Delta \gg J$ ). b) A homogeneous  $N$ -site ( $N \gg 1$ ) chain where the site-site coupling decays exponentially with distance. c) A schematic diagram of a two-generation three-fold dendrimer [19].

The optimization of energy transfer efficiency is thus simplified to the minimization of  $\langle t \rangle$ . It has been found that for many EET systems,  $\langle t \rangle$  decreases with increasing  $\Gamma$  for weak dissipation and diverges with  $\Gamma$  for strong dissipation, where  $\Gamma$  represents a characteristic dissipation strength in  $\mathcal{L}_{\text{dissp}}$ , e.g., the dephasing rate. [5–10]. A representative curve of this

dependence is plotted in Fig. 2a, where the trapping time  $\langle t \rangle$  is minimal at an optimal noise level  $\Gamma_{\text{opt}}$ . To understand this generic behavior, we investigate the asymptotic scaling of the trapping time in the strong and weak dissipation limits.

*Asymptotics of the trapping time.* — In the strong damping limit ( $\Gamma \rightarrow \infty$ ), quantum coherence is quickly destroyed by noise, and energy is transferred from donor sites to the trap through a series of incoherent hops. The hopping rate  $k_{\text{hop}}$  can be estimated from Fermi's golden rule,  $k_{\text{hop}} \sim |J|^2/\Gamma$ , where  $J$  is the exciton coupling strength. This relation is consistent with the Förster theory where  $\Gamma$  is proportional to the spectral line-width. The average trapping time diverges linearly with  $\Gamma$ , giving

$$\langle t \rangle \sim k_{\text{hop}}^{-1} \sim \Gamma/|J|^2. \quad (4)$$

In a recent paper, we mapped exciton dynamics to network kinetics using a systematic expansion and recovered hopping kinetics as the leading order term [9] in the strong damping limit. The exact  $\Gamma$ -dependence of the hopping rate  $k_{\text{hop}}$  is usually more complicated for a quantum non-Markovian description of dissipation. Nevertheless, the linear  $\Gamma$ -dependence of the trapping time in Eq. (4) can serve as a simple scaling relation for relative large values of damping[17].

In the opposite weak damping limit ( $\Gamma \rightarrow 0$ ), energy transfer can be enhanced by dynamic noise such that  $\langle t \rangle$  decreases with increasing  $\Gamma$ . Here the starting point for studying EET dynamics is the delocalized exciton basis, i.e., eigenstates of  $H_S$ , and energy is transferred coherently to the trap state through delocalized excitons. However, not every exciton state is capable of efficient energy transfer; a set of excitons, orthogonal to the trapping operator, define the trapping-free subspace  $\Phi_{\perp}$  (i.e., orthogonal subspace),

$$\mathcal{L}_{\text{trap}}\rho_{\perp} \cong 0, \quad (5)$$

where the index  $\perp$  denotes the trapping-free subspace such that  $\rho_{\perp} \in \Phi_{\perp}$ . Without the coupling to the trap, Eq. (5) indicates that the population in  $\Phi_{\perp}$  is conserved and therefore the coherent trapping time diverges,  $\langle t \rangle|_{\Gamma=0} = \infty$ . For a single trap site, the procedure of identifying  $\Phi_{\perp}$  has been provided in Ref. [8]. We note that Eq. (5) is analogous to the definition of decoherence-free subspace in quantum information, where the de-coupling from the system-bath interaction [16] is defined as the de-coupling from the system-trap overlap.

The system-bath coupling induces interactions between the trapping-free and other exciton states, thus leading to population depletion from the trapping-free subspace. Since

the population of the unperturbed orthogonal subspace will not deplete, dissipation of the orthogonal subspace  $\Phi_{\perp}$  dominates the population transfer time to the trap, giving  $(\mathcal{L}_0^{-1})_{\perp} \approx (\mathcal{L}_{\text{dissip};\perp})^{-1}$ , where  $\mathcal{L}_{\perp}$  represents the matrix element of the Liouville superoperator defined in  $\Phi_{\perp}$ . For nonzero population in  $\Phi_{\perp}$ , the leading order of the average trapping time is given by the survival time in the orthogonal exciton subspace,

$$\langle t \rangle \approx \text{Tr} [(l_{\text{dissip};\perp})^{-1} \rho_{\perp}(0)] / \Gamma, \quad (6)$$

where the linear form  $\mathcal{L}_{\text{dissip}} \approx \Gamma l_{\text{dissip}}$  is valid in the limit of  $\Gamma \rightarrow 0$ , and  $l_{\text{dissip}}$  is the reduced Liouville superoperator, independent of  $\Gamma$ .

*Generality.* — The two scaling relations in the asymptotic regimes are based on general physical arguments and thus independent of specific details such as the system-bath coupling, bath spectral density, truncation method, and approximations in the quantum master equation. Combining Equations (4) and (6), we obtain an estimation of the optimal condition,

$$\Gamma_{\text{opt}} \sim \left\{ \text{Tr} [(l_{\text{dissip};\perp})^{-1} \rho_{\perp}(0)] \right\}^{1/2} |J|, \quad (7)$$

which depends on the system Hamiltonian as well as the initial condition. In fact, the optimal efficiency or minimal trapping time is analogous to the Kramers turnover in reaction rate theory, where the two scaling regimes correspond to energy diffusion and spatial diffusion, respectively [20, 21]. The change of the reaction coordinate from energy to spatial position in classical rate theory corresponds to the change of basis set from excitons to local sites in energy transfer theory. However, the analogy to classical rate theory is limited to the orthogonal subspace and does not apply to the non-orthogonal subspace, where coherent energy transfer to the trap state is the dominant pathway in the weak damping limit and will not display noise-induced enhancement as illustrated in Fig. 2A.

The orthogonal condition in Eq. (5) for  $\Phi_{\perp}$  can be realized in various systems. (i) In an inhomogeneous system with large energy mismatches (see Fig. 1a), the orthogonality can arise from a vanishingly small overlap coefficient between the donor and acceptor. This situation can be well described by Fermi's golden rule and qualitatively explains the optimal efficiency observed in FMO [10, 18]. (ii) In a spatially extended system with a large number of sites, the orthogonality can arise because the average overlap coefficient of a local site with the trap decreases with the system size, e.g., a long, homogeneous chain system (see

Fig. 1b). (iii) In a system with intrinsic symmetry, each exciton state resulting from the diagonalization of  $H_{\text{sys}}$  is associated with a specific symmetry. A subset of these eigen-states are incompatible with the symmetry of the trapping Liouville operator  $\mathcal{L}_{\text{trap}}$ , thus leading to orthogonality. The fully-connected network [8] and the dendrimer in Fig. 1c are examples of such topological symmetry. The orthogonality due to symmetry in case (iii) is rigorous, whereas the orthogonality in cases (i) and (ii) requires either a large energy mismatch (i.e. detuning) or a large system size. In cases (i) and (ii), the average trapping time may not diverge at  $\Gamma = 0$  but can still lead to an optimal efficiency because of noise-enhancement under weak non-orthogonality.

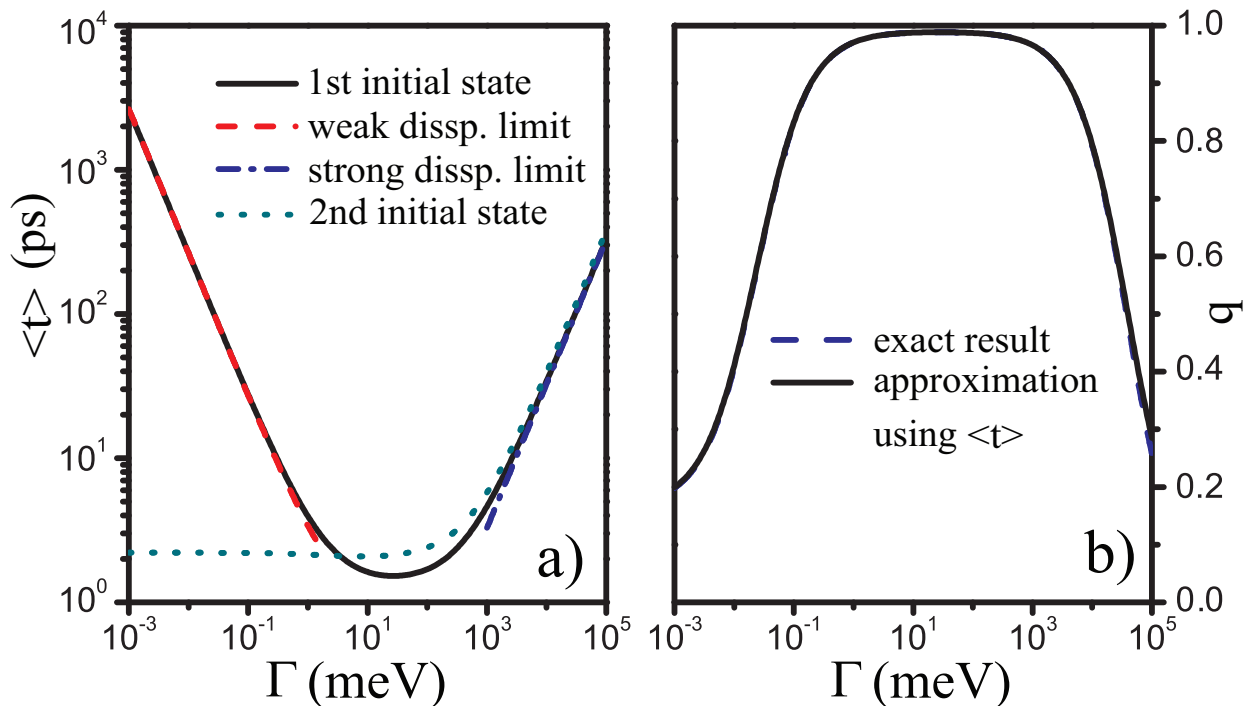


FIG. 2: EET in the dendrimer depicted in Fig. 1a. a) The trapping time  $\langle t \rangle$  vs. the pure dephasing rate  $\Gamma$ . For the incoherent initial condition defined at six outer 2nd-generation sites (i.e, the non-trapping state), the solid line is a full calculation. The dotted-dashed line is the large- $\Gamma$  result from Eq. (4). The dashed line is the small- $\Gamma$  result from Eq. (6). As a comparison, the dotted line is the result for the coherent initial condition defined at three 1st-generation sites (i.e, the trapping state). b) The transfer efficiency  $q$  vs.  $\Gamma$  for the 1st initial condition. The dashed line is the exact result as calculated from Eq. (2) while the solid line is obtained from the approximation in Eq. (3) and modification for  $\Gamma \lesssim 1$ . Here parameters are  $J = 20$  meV,  $k_t = 5$  meV, and  $k_d = 5$   $\mu$ eV.

*An example* — To verify the above analysis, we consider a two-generation three-fold dendrimer depicted in Fig. 1c [19]. A tight-bonding model is used for the system Hamiltonian, giving  $H_{S;ij} = \varepsilon_i \delta_{ij} |i\rangle\langle i| + J_{ij}(1 - \delta_{ij}) |i\rangle\langle j|$ , where  $|i\rangle$  represents a localized excited state at site  $i$ . All the site energies  $\varepsilon_i$  are assumed to be identical and the site-site interaction  $J_{ij} = 20$  meV is defined between two connected sites. The center site is the trap where the trapping process occurs with rate  $k_t = 5$  meV. The decay process is characterized by a homogeneous rate  $k_d = 5$   $\mu$ eV. For simplicity, we approximate dissipation by the Haken-Strobl-Reineker (HSR) model [22, 23] and consider homogeneous pure dephasing,  $\mathcal{L}_{\text{dissip};ij} = (1 - \delta_{i,j})\Gamma$ , where  $\Gamma$  is defined as the pure dephasing rate for each coherence element  $\rho_{ij}$ . For this dendrimer system, the symmetric Hamiltonian has an orthogonal subspace consisting of seven exciton states. We now compare two different cases of initial preparation. In the first case, an incoherent population is evenly distributed at six outer 2nd-generation sites, leading to  $\rho_{\perp}(0) \neq 0$ . The average trapping time is plotted as a function of the pure dephasing rate in Fig. 2a. The divergence of  $\langle t \rangle$  in the strong and weak dephasing limits is in an excellent agreement with the asymptotic behaviors predicted in Eqs. (4) and (6), respectively. Figure 2b shows that our approximate equation in Eq. (3) provides a quantitatively accurate description for the EET efficiency. Here a slight modification is applied in Eq. (3) to correct the zero-dissipation transfer efficiency [24]. In the second case, a coherent state is evenly distributed at three 1st-generation sites, leading to  $\rho_{\perp}(0) = 0$ . The small- $\Gamma$  divergence of  $\langle t \rangle$  in Eq. (6) disappears since no initial population exists in the orthogonal subspace. Above a threshold at the intermediate dephasing rate,  $\langle t \rangle$  changes from a plateau to the same linearly increasing function of  $\Gamma$ . This calculation confirms that dynamic noise can enhance the EET if the exciton subspace  $\Phi_{\perp}$  is orthogonal to the trapping process, and demonstrates the relevance of the initial condition for the energy transfer efficiency and thus the possibility of quantum control of energy transfer efficiency.

*Static disorder.* — We introduce an energy disorder  $\delta\varepsilon_i$  at each site  $i$ , that follows the Gaussian distribution,  $P(\delta\varepsilon_i) = \exp[-(\delta\varepsilon_i^2/(2\sigma_i^2))]/\sqrt{2\pi}\sigma_i$ , where  $\sigma_i$  is the variance of energy disorder. The resulting ensemble average is given by  $\langle x \rangle_{\sigma} = \Pi_i \int x(\delta\varepsilon_i)P(\delta\varepsilon_i)d\delta\varepsilon_i$  with  $x = \langle t \rangle$  or  $q$ . Using the above dendrimer model with the first initial condition, we present the results of  $\langle \langle t \rangle \rangle_{\sigma}$  and  $\langle q \rangle_{\sigma}$  obtained from a Monte Carlo simulation of  $10^5$  samples. As shown in Fig. 3a, static disorder is irrelevant in the strong dephasing limit ( $\Gamma \gg \sigma$ ). A more interesting  $\sigma$ -dependence occurs in the weak dephasing limit ( $\Gamma \ll \sigma$ ), where the trapping time is

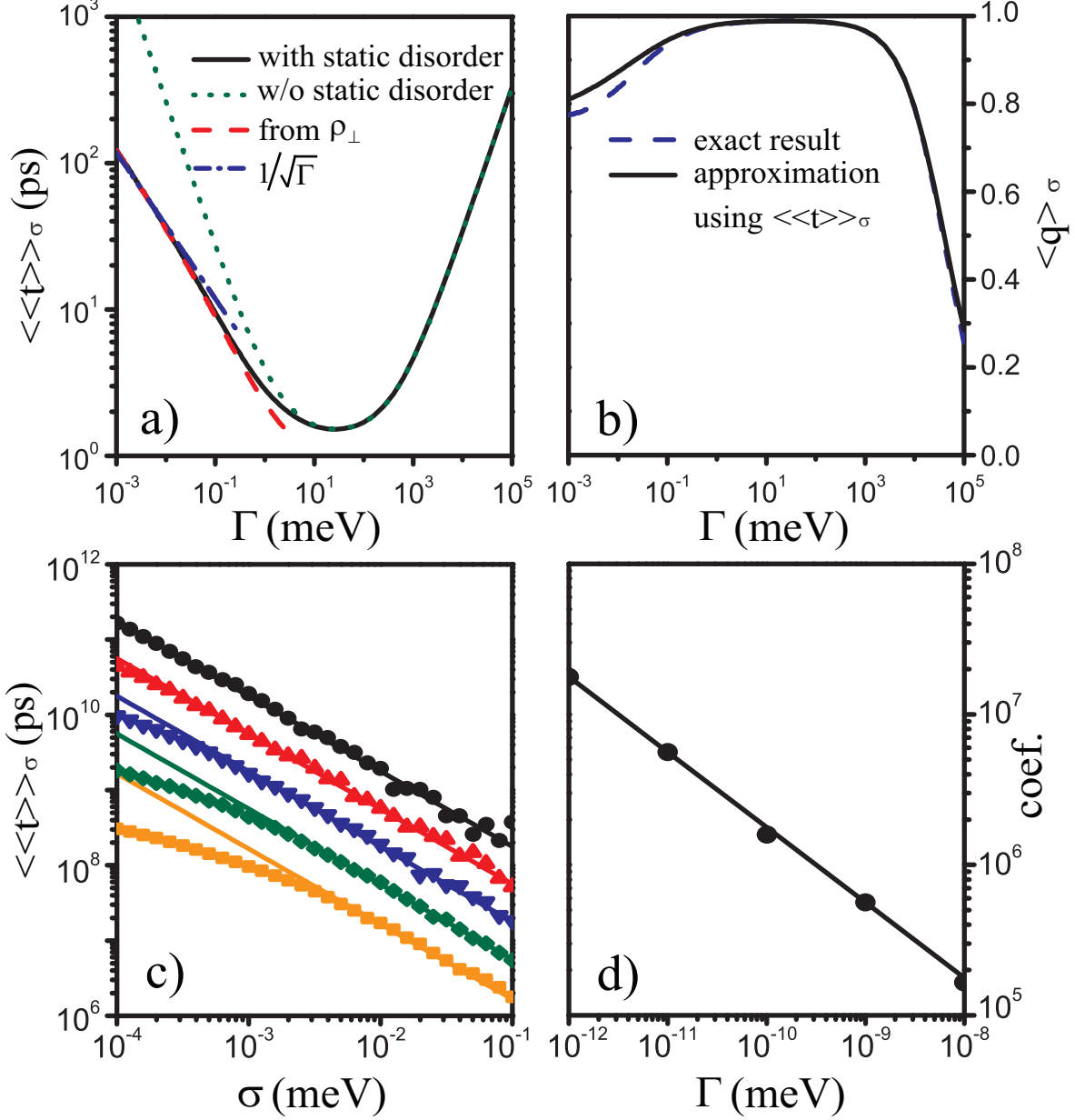


FIG. 3: The ensemble-averaged EET for the same dendrimer as in Fig. 2 with a static disorder  $\sigma = 4$  meV. a) The solid line is the simulation result of  $\langle\langle t \rangle\rangle_\sigma$ , referenced by the dotted line without  $\sigma$  from Fig. 2a. The dashed line is the dominant contribution from the orthogonal subspace, and the dashed-dotted line is the fitting result of  $1/\sqrt{\Gamma}$ . b)  $\langle q \rangle_\sigma$  vs.  $\Gamma$ : the solid line is the ensemble average of Eq. (2) whereas the dashed line is from Eq. (3) using  $\langle\langle t \rangle\rangle_\sigma$  and modification for  $\Gamma \lesssim 1$ . c) The weak-dephasing  $\sigma$ -dependence of  $\langle\langle t \rangle\rangle_\sigma$ , with  $\Gamma = 10^{-12}, 10^{-11}, 10^{-10}, 10^{-9}$ , and  $10^{-8}$  meV (from top to bottom). Symbols denote simulation results, whereas the solid lines are fitted with  $\langle\langle t \rangle\rangle_\sigma = c'/\sigma$ . d) The fitting coefficient  $c'$  (circles) is plotted as a function of  $\Gamma$  and can be further fitted by  $c' = c/\sqrt{\Gamma}$  (the solid line).



dominated by the survival time in the trapping-free subspace. Static disorder can destroy the orthogonality in Eq. (5) and induce a large reduction of the trapping time. However, if the random energy disorder falls below the amplitude of stochastic noise, the weak orthogonality is preserved and the trapping time diverges as  $\langle t \rangle \propto 1/\Gamma$ . Since the amplitude of the stochastic noise is proportional to  $\sqrt{\Gamma}$ , the range of relevant random energy that contributes to the divergence is defined by  $\sigma' \sim \sqrt{\Gamma}$ . Thus, we obtain the new asymptotic relation in the weak dephasing limit by an integral over these small disorders, giving

$$\langle \langle t \rangle \rangle_\sigma \sim \int_{-\sigma'}^{\sigma'} d\delta\varepsilon P(\delta\varepsilon) \langle t \rangle|_{|\delta\varepsilon| < \sigma'} \sim \frac{c}{\sigma\sqrt{\Gamma}}, \quad (8)$$

where  $\delta\varepsilon$  describes the effective in-phase energy fluctuation over all the sites,  $P(\delta\varepsilon) \sim 1/\sigma$  is the probability distribution, and  $\langle t \rangle|_{|\delta\varepsilon| < \sigma'} \approx \langle t \rangle|_{\delta\varepsilon=0} \sim 1/\Gamma$  is approximately uniform within this regime. The pre-factor  $c$  depends on the initial condition, the system Hamiltonian, and the trapping rate. We confirm the asymptotic relation,  $\langle \langle t \rangle \rangle_\sigma \propto 1/\sqrt{\Gamma}$ , by numerical fitting in Fig. 3a. Further, we calculate the weak-dephasing  $\langle \langle t \rangle \rangle_\sigma$  as a function of  $\sigma$  for different values of  $\Gamma$  in Figs. 3c-d and rigorously establish the scaling relation predicted by Eq. (8), i.e.,  $\langle \langle t \rangle \rangle_\sigma \propto 1/\sigma$ . Our calculations suggest that nature can use both static and dynamic disorders cooperatively to achieve efficient and robust energy transfer. Indeed, as shown in Fig. 3b, the zero dephasing efficiency  $\langle q|_{\Gamma=0} \rangle_\sigma$  is drastically enhanced from 0.2 to 0.8 with  $\sigma = J/5$ .

*Conclusion.* — In this Letter, we demonstrate that the generic mechanism of noise enhanced EET is to assist energy flow out of the orthogonal exciton subspace, and the competition between noise-enhanced EET in the weak dissipation regime and noise-induced localization in the strong dissipation regime leads to an optimal efficiency. We determine the scaling relations of the average trapping time in these two regimes and use the asymptotic relations to qualitatively predict the optimal noise. The presence of static disorder reduces the exponent of divergence in the weak-dissipation limit and thus makes the EET process more robust against noise. Our analysis is not limited to EET but also applies in general to electron transfer, fluorescence emission, heat conduction and other open quantum processes. Sophisticated numerical methods, such as the hierarchy equation approach, will be used to quantify the general optimal condition in the EET process. [17]

This work was supported by grants from the National Science Foundation (Grant CHE-1112825) and DARPA (Grant N66001-10-1-4063). JC is partially supported by the Center

for Excitonics funded by the US Department of Energy (Grant DE-SC0001088). JW acknowledges partial support from the Fundamental Research Funds for the Central Universities in China (Grant 2011QNA3005) and the National Science Foundation of China (Grant 21173185).

---

- [1] G. S. Engel, et. al., *Nature* **446**, 782 (2007).
- [2] H. Lee, Y. C. Cheng, and G. R. Fleming, *Science* **316**, 1462 (2007).
- [3] E. Collini, et. al., *Nature* **463**, 644 (2010).
- [4] G. Panitchayangkoon, et. al. *PNAS* **107**, 12766 (2010)
- [5] K. Gaab and C. Bardeen, *J. Chem. Phys.* **121**, 7813 (2004).
- [6] S. M. Vlaming, V. A. Malyshev, and J. Knoester, *J. Chem. Phys.* **127**, 154719 (2007)
- [7] P. Rebentrost, et. al., *New J. Phys.* **11**, 033003 (2009).
- [8] F. Caruso, et. al., *J. Chem. Phys.* **131**, 105106 (2009).
- [9] J. S. Cao and R. J. Silbey, *J. Phys. Chem. A* **113**, 13825 (2009).
- [10] J. L. Wu, F. Liu, Y. Shen, J. S. Cao, and R. J. Silbey, *New J. Phys.* **12**, 105012 (2010).
- [11] M. Sarovar, A. Ishizaki, G. R. Fleming, and K. B. Whaley *Nature Phys.* **6**, 462 (2010).
- [12] J. Moix, J. L. Wu, P. F. Huo, D. F. Coker, and J. S. Cao, *J. Phys. Chem. Lett.* **2**, 3045 (2011).
- [13] M. Mohseni, A. Shabani, S. Lloyd, and H. Rabitz, arXiv:1104.4812 (2011).
- [14] P. Brumer and M. Shapiro, arXiv:1109.0026.
- [15] T. Mancal and L. Valkunas, *New J. Phys.* **12** 065044 (2010).
- [16] D. A. Lidar, I. L. Chuang and K. B. Whaley, *Phys. Rev. Lett.* **81**, 2594 (1998).
- [17] We have obtained the detailed  $\Gamma$ -dependence of the trapping time in the two-state system and the FMO system using the hierarchy equation approach. Our results agree with the two scaling relations within the physically reasonable range of  $\Gamma$ .
- [18] J. L. Wu, F. Liu, J. Ma, R. J. Silbey, and J. S. Cao, arXiv:1109.5769.
- [19] C. Supritz, A. Engelmann, and P. Reineker, *J. Lumin.* **119**, 337 (2006).
- [20] J. E. Straub, M. Borkovec, and B. J. Berne, *J. Chem. Phys.* **84**, 1788 (1986).
- [21] E. Pollak, H. Grabert, and P. Hänggi, *J. Chem. Phys.* **91**, 4073 (1989).
- [22] H. Haken and P. Reineker, *Z. Physik* **249**, 253 (1972).
- [23] H. Haken and G. Strobl *Z. Phys.* **262**, 35 (1973).

[24] For small dephasing rates,  $\langle t \rangle$  is replaced by  $1/(\langle t \rangle^{-1} + t_0^{-1})$  in Eq. (3) where the constant  $t_0 = (q|_{\Gamma=0}^{-1} - 1)/k_d$  corrects the zero-dissipation transfer efficiency.